Kinetic theory of jamming in hard-sphere startup flows

R. S. Farr,[1,*] J. R. Melrose,[2,†] and R. C. Ball[1,‡]
[1]*Theory of Condensed Matter Group, Cavendish Laboratory, Madingley Road, Cambridge CB3 0HE, United Kingdom*
[2]*Polymer and Colloid Group, Cavendish Laboratory, Madingley Road, Cambridge CB3 0HE, United Kingdom*
(Received 25 July 1996; revised manuscript received 4 February 1997)

We consider the problem of hard spheres shearing from rest with hydrodynamic lubrication, but no Brownian forces. A theoretical model is presented, in terms of the aggregation of elongated clusters of particles, and predicts a jamming transition, where stress and average cluster size tend to infinity after a finite amount of strain. The model is compared with simulation data [Europhys. Lett. **32**, 535 (1995)], and predicts a critical volume fraction above which jamming will occur in macroscopic systems. [S1063-651X(97)01806-0]

PACS number(s): 47.50.+d, 83.50.−v

I. INTRODUCTION

A canonical problem in the rheology of colloids is the shear of a suspension of monodisperse hard spheres interacting hydrodynamically through a Newtonian solvent of viscosity η_0. We imagine the bulk material to be driven in simple shear by distant rheometer plates or, more elegantly, by Lees-Edwards boundary conditions [1] applied to an arbitrarily large periodic cell. The key issue in this paper is that for high enough volume fractions, a steady shear rate cannot be achieved. Shearing from rest, a logjam occurs at a finite strain angle.

For our system, the deformation rate is sufficiently small that inertial effects are negligible, that is, a Reynolds number defined on the particle diameter a is effectively zero. Stick boundary conditions hold at the particle surfaces. Hydrodynamics provides the only interactions; there are no Brownian, buoyancy, or other conservative forces, and indeed even the hard-sphere repulsion never actually affects the particles. This follows from the fact that the mobility for a pair of lubricating spheres falls to zero at contact so that the viscous solvent alone is sufficient to prevent particle overlap. The Péclet number Pe, defined by

$$\mathrm{Pe}=\frac{6\pi\dot{\gamma}\eta_0 a^3}{k_B T},$$

where $\dot{\gamma}$ is the rate of strain, is therefore formally infinite.

The problem of steady shear rate behavior has a venerable history starting with Einstein [2], who solved the case of infinite dilution, finding that the suspension viscosity η was increased over that of the solvent by a factor of $1+(5/2)\phi_v$ by the presence of hard spheres at a volume fraction $\phi_v \ll 1$. Following many phenomenological expressions at intermediate volume fractions, Frankel and Acrivos [3], assuming a cage model and lubrication interactions, proposed an expression for the viscosity close to the maximum packing limit ϕ_m, suggesting that it diverges close to this point as

$$\eta \propto \eta_0(1-\phi_v/\phi_m)^{-1}.$$

This result was supported theoretically by Nunan and Keller [4], who derived numerical results for periodic arrays of spheres, but was challenged as a result for continuously sheared random dispersions by Marrucci and Denn [5]. They argued that hydrodynamics could only provide a much weaker divergence, logarithmic in $(1-\phi_v/\phi_m)$, which is unable to account for the large viscosities observed experimentally in hard-sphere colloids. They further pointed out [5] that if hydrodynamics were to generate such large viscosities it must be via the formation of extended structures in the flow.

The arguments of [3] and [5] are mentioned here as they are both incorporated into the model presented in the next section; a context in which they are no longer irreconcilable.

Turning to computer simulations, Bossis and Brady [6], who approximated the hydrodynamics by a low order moment expansion and lubrication terms, indeed observed clustering among the particles in two dimensions. Ball and Melrose [7,8], who modeled the hydrodynamics by just retaining the lubrication terms and so were able to simulate much larger three-dimensional (3D) systems, found that the clusters (defined by a criterion on the gaps) consisted of irregular chains of particles forming along the compression axis, and growing until they hit their own periodic images. Since the code [8] rigorously imposed the no overlap constraint on the spheres, these percolating clusters locked up the system at a finite strain at which the stress should tend to infinity and the gaps in the cluster to zero. In practice the gaps collapsed catastrophically to below machine accuracy and so the simulations had to be stopped before the stress had grown by more than an order of magnitude.

This ''hydrodynamic logjam'' is an intrinsically many body effect in which gaps collapse more quickly than can be accounted for by any pair theory. The structures involved are, however, tied to the size of the simulation cell, which with current techniques is limited to of order 10^3 particles, so that in even the largest cells the clusters are still small, comprising no more than of order 10^1 particles. This leaves open the effect that clustering may have on a macroscopic system, but is suggestive that at $\mathrm{Pe}=\infty$ hard spheres will not flow; the response to an applied strain being transient and leading to a logjam.

*Electronic address: rsf10@phy.cam.ac.uk
†Electronic address: jrm23@phy.cam.ac.uk
‡Electronic address: rcb1@phy.cam.ac.uk

In this paper we present a model of the growth and aggregation of clusters upon shearing from rest, in an attempt to clarify the concept of the jam for an infinite system. The model provides predictions for a range of characteristics of the system, which may be tested against computer simulations and agree semiquantitatively for the early stages of the flow. We predict that above a lower critical volume fraction $\phi_l = 0.515 \pm 0.02$, the logjam is not confined to small systems, but occurs in macroscopic flows, being characterized by the formation of an infinite cluster before a strain of 1. Below this volume fraction we presume, but do not show, that steady flow may be achieved.

From the computer simulations it appears that achieving steady flow may be facilitated by repulsive conservative interactions between the particles [7]. These may be provided by polymer coats, particle deformability, or Brownian forces which from the second order Langevin equation lead to a repulsive interaction [7]. At present, the best model for the flow of hard spheres with hydrodynamic and Brownian forces is that due to Brady [9,10], who derives a pair theory from a truncation of the hierarchy of integral equations for the pair distribution function. He finds a viscosity which diverges close to maximum packing as

$$\eta \propto \eta_0 (1 - \phi_v / \phi_m)^{-2}, \tag{1}$$

in accordance with the standard phenomenological expression as found, for example, in [11], where $\phi_m \approx 0.63$ at low Pe and $\phi_m \approx 0.71$ for an ordered system at high Pe. This leading order divergence is due solely to the Brownian forces, one factor of $1/(1 - \phi_v / \phi_m)$ coming from the vanishing of the short time self-diffusivity, and the other from the divergence of the pair distribution function $g_2(r)$ at contact.

If this is true as claimed, for all Pe no matter how large, then it appears that the limit $\mathrm{Pe} \to \infty$ is qualitatively different to the case of $\mathrm{Pe} = \infty$. This receives backing from recent work of Brady [12] also in the context of a pair theory, who finds that at high Pe, boundary layers form in $g_2(r)$ in the compression directions when $r \approx a$. However, the pair theory is necessarily blind to any many body instabilities such as are considered here, and there is some evidence that a hydrodynamic jam of this type may be relevant to real systems at finite Pe and volume fractions substantially below the random close packed volume fraction $\phi_c \approx 0.63$ or the ϕ_m of Eq. (1). For example, D'Haene [13] observes a sudden *discontinuous* shear thickening (jump in stress) at high Pe in controlled strain rate experiments on hard spheres above a certain volume fraction, while Frith *et al.* [14] observe the same phenomenon in controlled stress experiments. Computer simulations [7] with conservative interparticle repulsion at finite shear rate scaled on this force are also prone to locking up. We suggest that our model of a hydrodynamic jam represents the physical mechanism underlying these observations. Once the jam gets under way, the stress is formally divergent and swamps the stress [Eq. (1)] due to continuous shear, although in the experimental systems, other effects such as particle deformability must intervene to curb this growth.

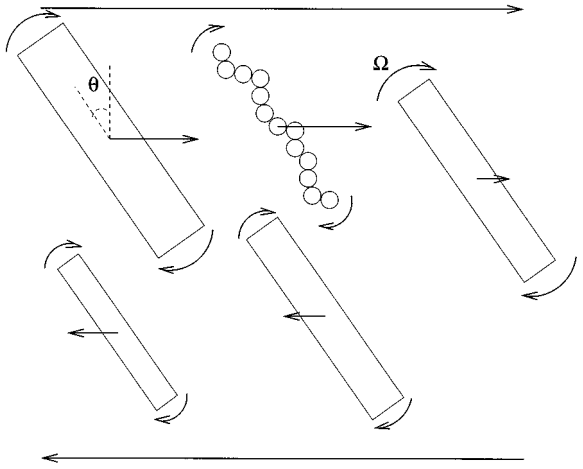

FIG. 1. Schematic picture of structures in the flow.

II. KINETIC MODEL

The principal structures in evidence in computer simulations of lubricating spheres [7] are irregular chains of nearly touching particles, which first form nearly parallel to the ''compression axis'' lying at 45° to the ''flow'' direction in the ''flow''-''gradient'' plane.

Figure 1 shows a schematic picture of the flow in which particles not belonging to the clusters are omitted. These clusters or rods of particles, forming at the start of the transient motion, are roughly parallel to one another and for simplicity we assume that all the rods which subsequently form and grow by aggregation constitute an approximately parallel population. It will turn out that this is a fairly consistent approximation as the jam occurs sufficiently quickly that any scatter in angles generated by the rotational component of the flow is minimal.

The rods contain extremely small interparticle gaps and are defined by this separation of length scales. We therefore take the rod lengths to be incompressible, and for a rod of j particles, each of diameter a, the length will be $L \approx ja$.

The bulk average deformation of the sample is simple shear; that is, a velocity field given by

$$\mathbf{v} = (0, 0, \dot{\gamma} x),$$

where the x, y, and z axes are the ''gradient,'' ''flow,'' and ''vorticity'' directions, respectively. We make a mean field approximation and imagine each rod to be embedded in this average flow, composed of the other rods, particles, and solvent. We further imagine that the rod translates and rotates as would a rigid line of zero thickness or a streak of material composing the mean flow. Thus its center of mass moves with the mean velocity at that point, and the rod rotates at angular velocity

$$\Omega = -\dot{\gamma} \cos^2 \theta, \tag{2}$$

where $\dot{\gamma}$ is the shear rate, and θ is the angle the rods make with the gradient direction, in the flow-gradient plane.

Viewed in a frame comoving and corotating with a rod, the surrounding mean flow is seen to be extension and compression along nonorthogonal axes (Fig. 2). This brings other rods towards it, tending to produce head to head collisions

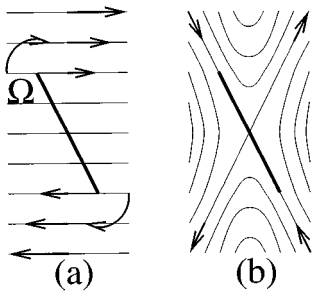

FIG. 2. (a) Mean flow field about a one dimensional rod immersed in a simple shear flow. (b) Same flow viewed in a frame corotating with the rod at angular velocity Ω [Eq. (2)]; as the rod does not fully corotate with the fluid, the apparent axes of compression and extension are not orthogonal.

and a new, longer rod. This growth by aggregation allows the large rods to rapidly increase in size and since the length of the rods determines their effect on the system, this in turn leads to a rapid increase in the bulk stress.

If we consider two rods about to collide, of lengths i and j particle diameters, respectively, we find that in this mean flow approximation, they approach one another with a relative velocity given by

$$V_{\mathrm{rel}}=\frac{\dot{\gamma}}{2}(ai+aj)\cos\theta\ \sin\theta.$$

In the collision we expect there to be some lateral offset. On a monomeric scale therefore, the transverse displacements of the particles from the long axis of the rod must form a two dimensional random walk. This fractal arrangement will necessarily be generated after repeated collision events.

The transverse span of the walk for j particles will be

$$W\propto aj^{1/2},$$

and so one might expect a collision cross section for two rods with spans W_1 and W_2 to be $\pi(W_1+W_2)^2$. This is problematical, since in the context of the aggregation equation to be presented below, it leads to an ''instantaneously gelling kernel'' [15]. It is clear, however, that this expression is an overestimate. The span of a walk is its maximum width at any point along its length; in fact, during a collision resulting in a longer rod, only a length of the order of the shorter of the two rods can become entangled. Thus a more reasonable estimate of the collision cross section Σ is

$$\Sigma=\omega_1[a\sqrt{\min(i,j)}]^2,$$

where ω_1 is a dimensionless constant, controlling the width of the walks.

If we now take the rod lengths to be approximately additive on collision, we will obtain a form of Smoluchowski's aggregation equation [16]:

$$\frac{dn_k}{dt}=\sum_{i,j}^{\infty}\ \Sigma V_{\mathrm{rel}}C(\phi_v)n_in_j(\delta_{i+j,k}-\delta_{i,k}-\delta_{j,k}). \qquad (3)$$

Here n_k is the number of rods per unit volume with length ka, and $C(\phi_v)$ is a ''crowding factor'' representing the increase in the collision frequency due to the volume excluded by the particles. Near the random close packed volume fraction $\phi_c\approx 0.63$ at which the dispersion is jammed at the start and cannot flow, one would expect the crowding factor to diverge as $1/[1-(\phi_v/\phi_c)^{1/3}]$. Note in Eq. (3) that the combinatorial factor of 1/2 normally present is canceled by the fact that rods may collide at both ends.

We may nondimensionalize in terms of $X_k=n_k/n_0$ where n_0 is the initial concentration of particles, and the scaled time

$$dT=dt\left(\frac{6\phi_v}{2\pi}\right)\dot{\gamma}\ \cos\theta\ \sin\theta C(\phi_v)\omega_1, \qquad (4)$$

where $\phi_v=\pi n_0a^3/6$, to obtain the standard form of Smoluchowski's equation [15]:

$$\frac{dX_k}{dT}=\frac{1}{2}\sum_{i,j}^{\infty}\ K_{ij}X_iX_j(\delta_{i+j,k}-\delta_{i,k}-\delta_{j,k}). \qquad (5)$$

This has the homogeneous kernel

$$K_{ij}=2(i+j)\min(i,j)=2ij+2[\min(i,j)]^2. \qquad (6)$$

In the notation of Van Dongen [15] this kernel has scaling exponents $\lambda=2$ and $\mu=\nu=1$, which places it in the class that undergoes a gel transition where the average cluster size tends to infinity after a finite amount of reduced time. Van Dongen also derives scaling solutions applying close to this gel point, and in particular, we have the divergence in the third moment of the cluster size,

$$M_3=\sum_{j=1}^{\infty}\ j^3X_j\sim(1-T/T_{\mathrm{gel}})^{-3}, \qquad (7)$$

which we will show later, gives the asymptotic form of the stress close to the hydrodynamically jammed state. It is also important that the buildup of this divergence results from aggregation among the larger prevailing rods [17]; this justifies our earlier neglect, in discussing Eq. (3), of events where a long rod captures shorter ones without increasing in length, since the short rod population is relatively unimportant.

For our purposes, we will also need an explicit solution to Eq. (5), which will require the initial rod orientation. This is taken to be $\theta_0=\pi/4$, being a ''typical'' angle of first collision, and the orientation for which rod growth in this model is fastest (so that if rod growth starts in various directions, this one is singled out by the kinetics).

III. SOLUTION OF SMOLUCHOWSKI'S EQUATION

We approach the set of Eqs. (5) by obtaining the Taylor series solution about the origin, for monomeric initial conditions $[X_1(T=0)=1]$.

Van Dongen [15] provides the first term in the expansion for each cluster size:

$$X_n=N_nT^{n-1}+O(T^n),$$

where the numbers N_n are given by the recurrence relation:

$$(n-1)N_n=\frac{1}{2}\sum_{i+j=n} K_{ij}N_iN_j\,.$$

This is readily generalized, to provide the full Taylor expansion, up to a given order, for

$$X_n(T)=\sum_k x_n^{[k+1]}T^k.$$

With $x_1^{[1]}=1$, and $x_a^{[b]}=0 \;\; \forall a>b$, then

$$(k+r-1)x_k^{[k+r]}=\frac{1}{2}\sum_{a=1}^{k-1}\left[K_{a,k-a}\sum_{c=0}^{r} x_{k-a}^{[k+r-a-c]}\right] - \sum_{c=0}^{r-1}\left[x_k^{[k+c]}\sum_{m=1}^{r-c} K_{km}x_m^{[r-c]}\right]. \quad (8)$$

This is used by first setting $r=0$, and applying the formula, for $k=1,2,\ldots$, then proceeding to $r=1$, etc. filling in the matrix of coefficients in a diagonal manner.

The Taylor expansion of any desired moment is then obtained trivially.

For reasons to follow, we are interested in the third moment of the cluster size; a Domb-Sykes plot shows this to have an unphysical nonpolar singularity, at $T\approx -0.093$, so to obtain a solution out to the gel point, a continued fraction expansion was derived from the Taylor series. This has the advantage of being able to reproduce subtle analytic properties of the solution [18]; building branch cuts out of alternating poles and zeroes radiating from the origin of the complex T plane, and placing polar singularities, in roughly the right position, as the order increases.

For the kernel in Eq. (6), pole zero plots were drawn, for the continued fraction expansion of M_3, using up to 50 Taylor terms. A cluster of three poles was observed, which converged towards $T\approx 0.33$ as the order was increased, in accordance with Van Dongen's scaling results. This value is somewhat less than the gel time of 0.5 for the product kernel $K_{ij}=2ij$, as would be expected from the form of Eq. (6).

IV. JAMMING AND THE BEHAVIOR OF THE STRESS

To calculate the stress, we imagine the rods to be immersed in the mean effective fluid composed of the other rods, particles, and solvent. From Fig. 2, we see that in the corotating frame of a thin rod, the velocity of the background flow relative to the rod and close to it is parallel to this rod and increases linearly with distance from the center of mass. Let x be this distance; then the relative speed is readily shown to be

$$v=\dot{\gamma}(\sin\theta)(\cos\theta)x. \quad (9)$$

In the mean field approximation this passing fluid exerts a frictional force per unit length dF/dx given by

$$\frac{dF}{dx}=E(\phi_v)\,\dot{\gamma}(\sin\theta)(\cos\theta)x, \quad (10)$$

where $E(\phi_v)$ is a parameter for each volume fraction, with the dimensions of viscosity.

From this ansatz and Eq. (8), we readily calculate the viscous power dissipated around a rod of j particles, as

$$\int_{-ja/2}^{ja/2} E(\phi_v)[\dot{\gamma}(\sin\theta)(\cos\theta)x]^2dx$$

and therefore the stress $\sigma_{\rm rod}$ in the fluid due to the rods (which contain at least two particles) is

$$\sigma_{\rm rod}=\frac{E(\phi_v)}{12}\dot{\gamma}(\cos^2\theta)(\sin^2\theta)\left(\frac{6\phi_v}{\pi}\right)\sum_{j=2}^{\infty} j^3X_j\,. \quad (11)$$

Since from Eq. (7) this stress will dominate at late times, the model predicts that colloids with purely hydrodynamic interactions can jam up, after a finite amount $\gamma_{\rm jam}$ of strain, with the stress diverging with the third moment of the cluster size, that is, as $(\gamma-\gamma_{\rm jam})^{-3}$ close to this point.

In this model, the condition for jamming is that the reduced time reaches a value of $T_{\rm gel}=0.33$, before the rods ''tumble'' by reaching $\theta=0$ and are no longer subject to a compressional flow field (Fig. 2).

We expect our discussion above to apply quantitatively close to the jamming point; unfortunately computer simulations are restricted to the initial phase of the flow, where we can no longer assume that the stress is dominated by large rods. These rods, once they form, will have disrupted the local affine flow, carving out ''channels'' in the effective fluid, in which their constituent particles may have large velocity components in the ''gradient'' direction. In contrast the monomers, whose contribution to the stress is omitted from Eq. (11), will by and large partake of the average affine flow.

The monomers will dissipate a power P given by

$$P=\sigma_{\rm mon}\dot{\gamma}=n_b\langle P_b\rangle, \quad (12)$$

where n_b is the concentration of actively deforming nearest neighbor bonds, and $\langle P_b\rangle$ is the average power dissipated by such a bond. Initially, when the stress in the dispersion is $\sigma(0)$, we will have $n_b=(1/2)\nu_{\rm NN}n_0$ where $\nu_{\rm NN}$ is the number of nearest neighbors per particle, and is approximately 10 near to random close packing.

At later times, some of the monomers have been incorporated into rods, and so one might expect

$$\sigma_{\rm mon}\approx X_1\sigma(0) \quad (13)$$

so that the final expression for the stress is

$$\sigma=\sigma_{\rm mon}+\sigma_{\rm rod}\,, \quad (14)$$

which involves the three parameters ω_1, $E(\phi_v)$, and $\sigma(0)$, theoretical estimates of which will be given below.

It must be pointed out that the form of Eq. (13) is rather arguable, depending upon how many gaps around and within a rod one considers to be either no longer active in dissipating power, or to have been counted by Eq. (10). Most of the results that follow, and in particular the ''lower critical volume fraction'' ϕ_l, are somewhat sensitive to the details of this equation; for example, the fitted values of $E(\phi_v)$ are most sensitive, and may vary by as much as a factor of 2 upon making different assumptions.

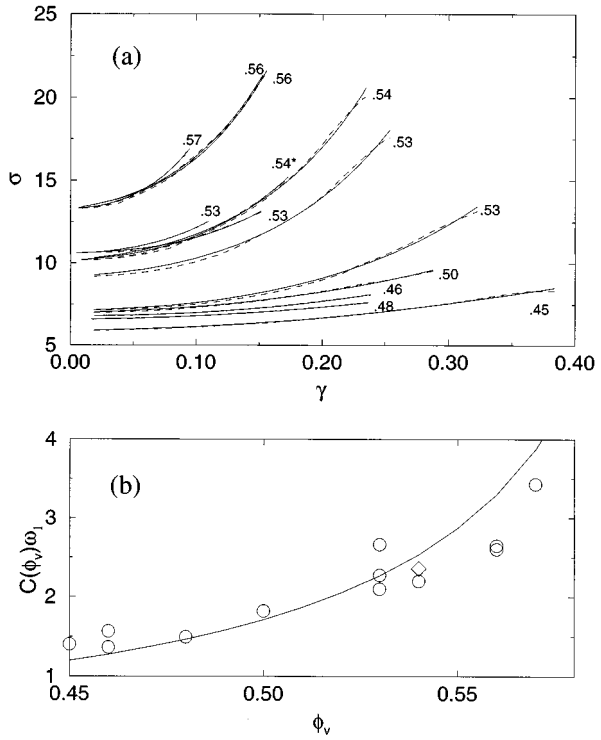

FIG. 3. (a) Simulation (dashed), and fitted theoretical (solid) graphs of σ against γ, at the 13 volume fractions indicated next to the curves. For this and the following figures units are chosen so that $a=\eta_0=1=\dot{\gamma}$: Thus the physical stress σ is in units of $\eta_0\dot{\gamma}$. (b) Fitted values of the product $C(\phi_v)\omega_1$, where the diamond is for 1400 particles. The solid line is a fit to Eq. (15) in the text.

To test Eq. (14), computer simulations involving pure hydrodynamic interactions were run, for several volume fractions and 700 particles, in an initially cubic simulation cell, using the code of Ref. [8]. The resulting stress vs strain curves, were fitted to Eq. (14), by choosing $E(\phi_v)$, and the product $C(\phi_v)\omega_1$ for each volume fraction as shown in Fig. 3(a). The simulation results at each volume fraction are shown dashed, and the fitted theoretical results, which in each case lie essentially on top of the simulation data, are shown as solid curves. Figure 3(b) shows the best values of the product $C(\phi_v)\omega_1$ as a function of ϕ_v, and a fit to the form

$$\frac{\omega_1}{1-(\phi_v/\phi_c)^{1/3}}, \tag{15}$$

where ω_1 is constant for all ϕ_v ($\omega_1=0.13\pm0.02$ fits best). This value of ω_1 is *a priori* reasonable, since the step size of the random walk in particle diameters is then of order $\omega_1^{1/2}\approx 0.35$.

Since we are dealing with large scale structures in the flow, finite size effects may well be important. To test their significance, a 1400 particle simulation was run, in an initially cuboidal simulation cell of aspect ratio 1:1:2—the longer side being in the flow direction, and this geometry chosen to reduce the risk of a growing cluster hitting one of its periodic images. The results are shown alongside the 700 particle runs in Figs. 3 and 5, and the model is able to fit them, with essentially the same values for the parameters.

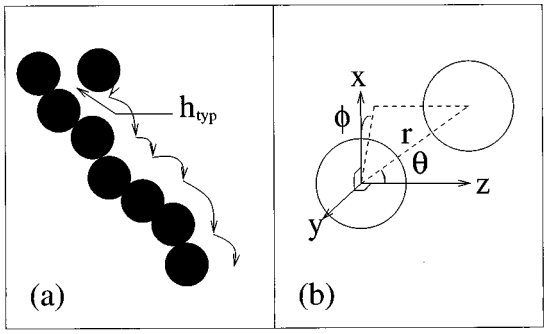

FIG. 4. (a) Schematic picture of a particle sliding along a cluster in the flow, generating the friction parameter $E(\phi_v)$. (b) Two particles in general position, with centers separated by a distance $r\approx a+h_{\rm typ}$.

V. ESTIMATES OF THE MODEL PARAMETERS

So far, the values of $E(\phi)$ and $\sigma(0)$ have simply been extracted from the simulation data; however, we do have some theoretical handle upon them. Consider first a typical gap between nearest neighbors; this falls to zero at random close packing, and considering the low concentration limit, one readily sees that a reasonable estimate is

$$h_{\rm typ}\approx a\left(\frac{\pi}{6}\right)^{1/3}\left[\left(\frac{1}{\phi_v}\right)^{1/3}-\left(\frac{1}{\phi_c}\right)^{1/3}\right], \tag{16}$$

which vanishes as $(1-\phi_v/\phi_c)^{-1}$ near ϕ_c.

To estimate the value of $E(\phi_v)$ we follow an argument similar to Marrucci and Denn [5], and imagine a particle in the effective fluid sliding along the cluster [Fig. 4(a)] with a relative speed v [Eq. (9)] and maintaining a distance $h_{\rm typ}$ from it. When it separates from one of the particles in the cluster to move to the next, the gap will change roughly as $h=h_{\rm typ}+vt$, and so the impulse along the separation direction, from the instantaneous ''squeeze'' force F, is

$$\mathcal{I}=\int F\ dt=\int_{t=0}^{a/v}\frac{3\pi\eta_0 v a^2}{8h}dt.$$

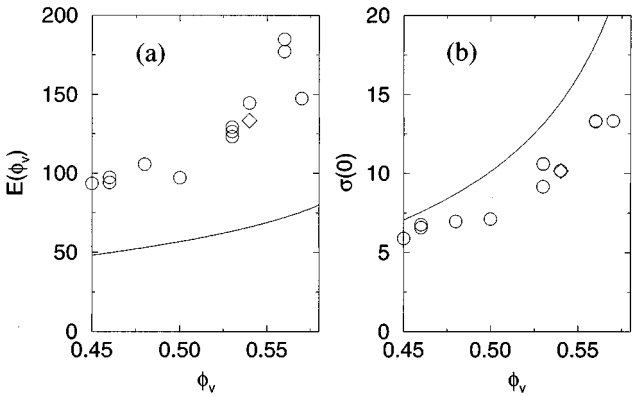

FIG. 5. (a) Plot of $E(\phi_v)\eta_0$ against ϕ_v obtained from the fit to the stress-strain data in Fig. 3. The circles for 700 particles and the diamond for 1400 particles show good agreement. The solid line for comparison is a theoretical prediction [Eq. (17) in the text]. (b) Same for $\sigma(0)\dot{\gamma}\eta_0$; the theoretical prediction is from Eq. (18).

The rate of encounter of particles in the cluster is a/v and if we assume each particle of the rod has eight particles sliding past, and that $a \gg h_{\mathrm{typ}}$, then the sliding force on a length a of the rod due to squeeze lubrication interactions is

$$F_{\mathrm{sq}} = 8\mathcal{I}\frac{v}{a} \approx 3\pi\eta_0 a v \ \ln\left(\frac{a}{h_{\mathrm{typ}}}\right).$$

This force is logarithmic in the gap, and so one needs to include the logarithmic ''shear'' lubrication forces of the sliding particles, which contribute

$$F_{\mathrm{sh}} = 8\frac{\pi\eta_0 a v}{2}\ln\left(\frac{a}{2h_{\mathrm{typ}}}\right)$$

for a length a of the rod. When compared with Eq. (10) this gives, ignoring factors of order unity inside the logarithm,

$$E(\phi_v) \approx 7\pi\eta_0 \ln\left(\frac{a}{h_{\mathrm{typ}}}\right). \tag{17}$$

Figure 5(a) shows the fitted values of $E(\phi_v)$ from the simulation plotted with this theoretical prediction, and shows that Eq. (17) underestimates the fitted values, by a factor of about 2. This is quite acceptable for an argument based purely on dimensional grounds, and indeed, one might expect an underestimate on the part of Eq. (17), since we have assumed that all gaps surrounding the rods are of size h_{typ}, while in practice, the rod will have to fight through many gaps that are significantly smaller than this.

Next we turn to $\sigma(0)$, which is the stress at the moment the simulation is started. Consider two particles, as in Fig. 4(b), moving with the affine flow, and separated by a position vector given in polar coordinates by

$$\mathbf{r} = \begin{pmatrix} r\ \sin\theta\ \cos\phi \\ r\ \sin\theta\ \sin\phi \\ r\ \cos\theta \end{pmatrix},$$

Where the gradient, vorticity, and flow directions are the x, y, and z axes, respectively, and $r \approx a + h_{\mathrm{typ}}$. The relative velocity of the particles is therefore

$$\mathbf{v}_{\mathrm{rel}} = \dot{\gamma} r (\sin\theta)(\cos\phi)\hat{\mathbf{z}}.$$

The ''squeeze'' and ''shear'' components of this are

$$|v_{\mathrm{sq}}| = \dot{\gamma} r\ \sin\theta\ \cos\theta\ \cos\phi,$$

$$|v_{\mathrm{sh}}| = \dot{\gamma} r\ \sin^2\theta\ \cos\phi,$$

and so the power dissipated in the bond will be

$$\langle P_b \rangle = \frac{3\pi\eta_0 a^2}{8h_{\mathrm{typ}}}\langle v_{\mathrm{sq}}^2 \rangle + \frac{\pi\eta_0 a}{2}\langle v_{\mathrm{sh}}^2 \rangle,$$

where the angle brackets denote an average over all orientations with equal weight.

This leads from Eq. (12) to

$$\sigma(0) \approx \frac{3\phi_v \nu_{\mathrm{NN}} \dot{\gamma}^2}{a^3\pi}(a + h_{\mathrm{typ}})^2\left[\frac{\pi\eta_0 a^2}{40h_{\mathrm{typ}}} + \frac{2\pi\eta_0 a}{15}\ln\left(\frac{a}{2h_{\mathrm{typ}}}\right)\right], \tag{18}$$

which, as discussed shortly, diverges near random close packing as $(1 - \phi_v/\phi_c)^{-1}$.

This prediction is plotted with the actual values from the simulation data in Fig. 5(b) and shows that the agreement is reasonable, given the crudeness of the approximations.

The derivation of Eq. (18) is essentially that due to Frankel and Acrivos [3] who intended to predict the steady state rheology of a concentrated dispersion. As pointed out by Marrucci and Denn [5], the argument makes the implicit assumption that

$$\left\langle \frac{v^2}{h} \right\rangle \approx \frac{\langle v^2 \rangle}{\langle h \rangle}, \tag{19}$$

where v is the relative velocity of a pair of particles and the average is performed over all nearest neighbor pairs in the system. This is unjustified at late times, when the velocities and gaps will be highly correlated [5]. In our case we apply the argument only at the start of the flow, when the gaps are prescribed by the initial configuration and Eq. (19) is a fair approximation.

Equations (17) and (18) together with the reasonable guess that $\omega_1^{1/2} \approx 0.5$, or a little less, therefore provide a semiquantitative description of hydrodynamic jamming with no free parameters.

Although these parameters may be predicted theoretically, the lower critical volume fraction ϕ_l derived in Sec. VII below is obtained from a fit to simulation data, and is not dependent on Eqs. (17) and (18).

VI. CLOSURE OF THE SMALLEST GAPS

Given the $E(\phi_v)$'s and products $C(\phi_v)\omega_1$ fitted to Eq. (14), the dynamics of the infinite system are determined and it should be possible to calculate the distribution of gap sizes as a function of strain γ. In practice, however, this is a difficult problem as it involves taking an average over all the possible histories of gaps lying in rods (a possibility space of very large dimension) while the solution of Sec. III only gives us access to the populations of different rod lengths as a function of strain. Instead, we are forced to make an estimate based on a scaling argument.

We start by noting that in the model, there is a typical longest rod length, which will scale as

$$L_{\mathrm{max}} = \lambda a (1 - T/T_{\mathrm{gel}})^{-2} \tag{20}$$

for some factor λ, of order unity (λ is likely to be system-size dependent). We then assert that the smallest gaps have always been near the center of a rod of this typical maximum size. Such a gap, h, will be squeezed by the compressive force F_c in the rod, so that

$$\dot{h} = -\frac{8hF_c}{3\pi\eta_0 a^2}, \tag{21}$$

and so, using Eq. (10) we obtain an expression for the minimum gap:

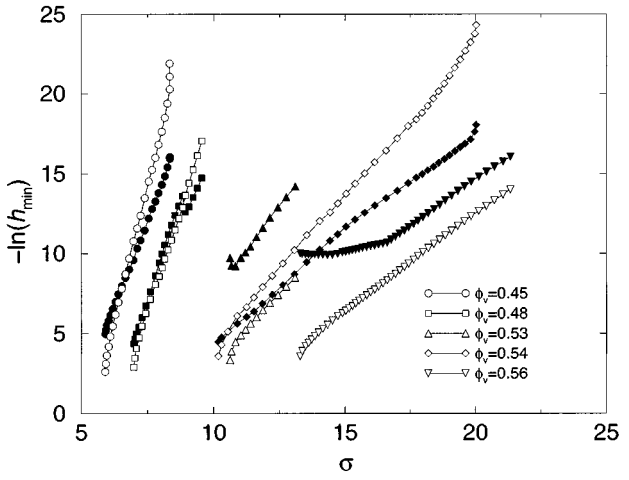

FIG. 6. Simulation, and theoretical curves of $-\ln(h_{\min}a)$ against $\sigma\eta_0\dot{\gamma}$, for various ϕ_v with $\lambda=2.1$. The open symbols show fitted theoretical results [Eq. (22)], and the closed symbols of the same shape are the simulation data at the same volume fraction.

$$-\ln\left[\frac{h_{\min}}{h_{\min}(0)}\right]=\frac{\lambda^2E(\phi_v)}{9C(\phi_v)\ \omega_1\eta_0\phi_v}[(1-T/T_{\rm gel})^{-3}-1]\frac{T_{\rm gel}}{3}. \tag{22}$$

We may also (over) estimate the size of the initial minimum gap $h_{\min}(0)$ (which will be highly sample dependent) from

$$h_{\min}(0)\approx h_{\rm typ}.$$

The model thus predicts that the smallest gap will collapse catastrophically, falling as $\exp[(\gamma-\gamma_{\rm jam})^{-3}]$ near the gel point. It is this singular dependence which makes computer simulations of this regime extremely difficult. However, it also has a bearing on the self-consistency of the model, for the rods are only defined by a separation of length scales, between gaps and particle diameters. A rapid collapse of the gaps is therefore essential to this approximation.

Figure 6 shows $-\ln h_{\min}$ plotted against the stress σ, for simulations of 700 particles and the predicted curves superposed at various volume fractions. A value of 2.1 was used for λ.

VII. LOWER CRITICAL VOLUME FRACTION

Our model predicts a lower volume fraction ϕ_l below which the rods will tumble (reaching $\theta=0$ and $\gamma=1$) before the gel transition occurs (at $T=T_{\rm gel}\approx 0.33$). Since the reduced time T is related to the angle θ the rods make with the gradient direction, by [Eqs. (2) and (4)]

$$T=\frac{6\phi_v}{2\pi}\dot{\gamma}C(\phi_v)\omega_1\ln\left(\frac{\cos\theta}{\cos\theta_0}\right),$$

with $\theta_0=\pi/4$, it follows from Eq. (15) and the fitted value of ω_1 that $\phi_l=0.515\pm0.015$. It should be noted, however, that the error on ϕ_l is only in the context of the precise model presented here; its value is quite sensitive to the detailed assumptions made about, e.g., the form of the stress [Eq. (13)].

We suggest that this concept of a lower critical volume fraction ϕ_l may be of relevance to sudden shear thickening in real colloids, with finite values of Péclet number. D'Haene [13], for example, finds that in controlled strain rate experiments on hard-sphere systems, there is a discontinuous jump in stress as a function of Pe, but only above a volume fraction of 53–54 %. In the context of our model, this would correspond to the onset of a jammed state, with the formation of system spanning clusters leading to the irregular stress fluctuations he observes after the discontinuous thickening. Since the stress he observes does not grow arbitrarily, the consequences of this putative logjam must be mitigated in his experiments by some other effect such as particle deformation or fracture.

VIII. CLUSTERS IN THE SIMULATION

The computer simulations contain all the information about the flow, and so can be used to visualize, and perform statistics on any structures that may be present. In order to define a cluster, we choose a criterion based upon interparticle gaps, which is that two particles belong to the same cluster if they are separated by a gap h less than some critical gap h_c, for which we take a ''theory-driven'' value. In the context of this theory, we choose for h_c a value dependent upon the expected gap h_d in a dimer forming at the start of the flow. This is predicted to collapse like

$$h_d=h_{\rm typ}\exp\left[\frac{2E(\phi_v)}{3\pi\eta_0}\ln\left(\frac{\cos(\pi/4)}{\cos\theta}\right)\right], \tag{23}$$

in which the time dependence enters through θ, and we take

$$h_c=\frac{h_d}{\beta}, \tag{24}$$

where β is some parameter of order unity.

A simulation was run at $\phi_v=0.53$, using 700 particles and $E(\phi_v)=125$, and the configurations partitioned into clusters on the basis of Eq. (23). From these partitions we may define moments of the cluster sizes: Let $\mathcal{P}_j$ be the fraction of particles belonging to clusters of size j particles, then we define the qth moment M_q by

$$M_q=\sum_{j=1}^{\infty}\mathcal{P}_j\ j^q.$$

Figure 7 shows plots of M_2 and M_3, averaged over various strain intervals, as a function of strain, γ for five values of β. The error bars show the predicted values, using $\omega_1=0.13\pm0.02$.

Lastly, in order to obtain some pictorial impression of these clusters, six configurations equally spaced in strain were chosen from this simulation at $\phi_v=0.53$ using $\beta=3$. The clusters in the flow were then analyzed by finding for each the ''radius of gyration'' tensor $\mathcal{R}$. This is defined in the following manner: Let k label each of the N particles belonging to the cluster in turn. Let $\mathbf{r}_k$ be the position vector of the kth particle and

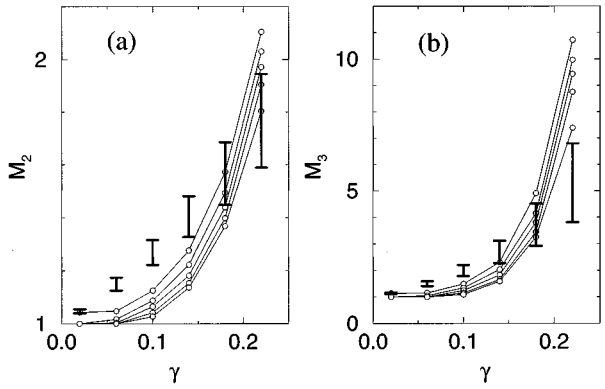

FIG. 7. (a) Plot of M_2 against strain γ for the five values $\beta = 2.6, 3.0, 3.5, 4.0, 4.5$. Each point in strain is actually an average over four equally spaced configurations in one of the six strain ranges, $\gamma=0-0.04$, $0.04-0.08$, $0.08-0.12$, $0.12-0.16$, $0.16-0.20$, and $0.20-0.24$. The six error bars show the predicted values of the moment M_2, for each strain range, using $\omega_1=0.13\pm0.02$. (b) Same for M_3.

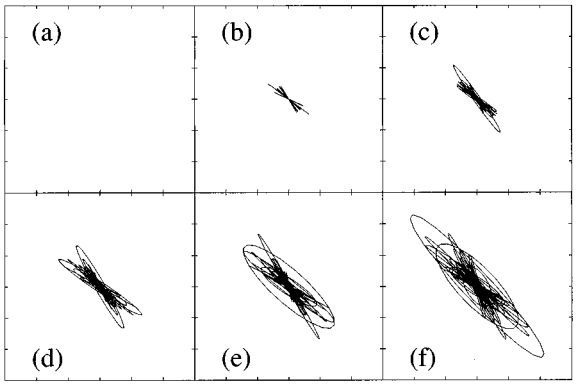

FIG. 8. Plots of projections of the ellipsoids from Eq. (25) for all the clusters in a configuration. Tick marks on the axes are at a spacing of one particle diameter. Configurations are at (a)–(f) $\gamma=0.04$, 0.08, 0.12, 0.16, 0.20, and 0.24.

$$\mathbf{r}_{\text{c.m.}}=\sum_k \mathbf{r}_k/N$$

the center of mass of the cluster. Then

$$\mathcal{R}=\sum_k \frac{(\mathbf{r}_k-\mathbf{r}_{\text{c.m.}})(\mathbf{r}_k-\mathbf{r}_{\text{c.m.}})}{N}.$$

This tensor defines an ellipsoid approximating the cluster's true distribution in space. To project this ellipsoid onto the flow-gradient plane, let the x, y, and z axes be the flow, gradient, and vorticity directions, then define a new 2 by 2 tensor $\mathcal{R}_P$, by the upper left hand corner of $\mathcal{R}$. The projection onto the plane $z=0$ is then the set of points $\{\mathbf{x}\}$ given by

$$\mathbf{x}=\mathcal{R}_P^{1/2}\hat{\mathbf{n}}, \tag{25}$$

where $\hat{\mathbf{n}}$ is a vector lying on the unit circle in the plane $z=0$.

These projections are plotted for the chosen configurations in Fig. 8, and clearly show narrow ''rods'' near the ''compression'' axis ($\theta=\pi/4$). However, since Fig. 8 suppresses all information about the ''vorticity'' direction, one may wonder how good is the approximation that the rods are confined to the $z=0$ plane. This was tested, by calculating the average value, and standard deviation of the vector representing the principal axis of each ellipsoid. We find that this vector has a component in the vorticity direction with a mean of less than 0.02 particle diameters, and a standard deviation increasing from $0.10a$ at $\gamma=0.08$ to $0.22a$ at $\gamma=0.24$, entirely consistent with the clusters lying in the flow-gradient plane.

IX. CONCLUSION

In this paper we have constructed a model of the stress carrying ''fabric'' in a concentrated dispersion of hard spheres at $\text{Pe}=\infty$. The model predicts that above a lower volume fraction ϕ_l substantially less than 0.63, a hydrodynamic logjam occurs even in an infinite system. This is characterized by an elongated cluster or rod, first forming parallel to the compression axis, growing to infinite size before it tumbles by passing $\theta=0$ and entering a region of extensional flow. The model quantifies the hitherto qualitative notion of hydrodynamic clustering and jamming, which we believe to be a new physical phenomenon underlying discontinuous shear thickening.

At volume fractions below ϕ_l, the clusters in the model will tumble, passing $\theta=0$ and failing to jam at a ''first attempt.'' The assumption that all clusters in the flow remain roughly parallel will then break down, as it is closely tied to the transience of the motion. Whether a steady state is then eventually achieved is not covered by our model and remains an open question. It is therefore unclear whether for a pure hydrodynamic model a divergence such as Eq. (1) can be studied below ϕ_l.

ACKNOWLEDGMENT

Thanks are due to Dr. C. Nex, for his help and advice on Padé approximants.

[1] A. W. Lees and S. F. Edwards, J. Phys. C **5**, 1921 (1972).
[2] A. Einstein, Ann. Phys. (Leipzig) **19**, 289 (1906).
[3] N. A. Frankel and A. Acrivos, Chem. Eng. Sci. **22**, 847 (1967).
[4] K. C. Nunan and J. B. Keller, J. Fluid. Mech. **142**, 269 (1984).
[5] G. Marrucci and M. M. Denn, Rheol. Acta **24**, 317 (1985).
[6] G. Bossis and J. F. Brady, J. Chem. Phys. **80**, 5141 (1984).
[7] R. C. Ball and J. R. Melrose, Adv. Colloid Interface Sci. **59**, 19 (1995).
[8] J. R. Melrose and R. C. Ball, Europhys. Lett. **32**, 535 (1995).
[9] J. F. Brady, J. Chem. Phys. **99**, 567 (1993).
[10] J. F. Brady, J. Fluid Mech. **272**, 109 (1994).
[11] W. B. Russel, D. A. Saville, and W. R. Schowalter, *Colloidal*

Dispersions (Cambridge University Press, Cambridge, England, 1989).
[12] J. F. Brady (private communication).
[13] P. D'Haene, Ph.D. thesis, Katholieke Universitiet Leuven, 1992.
[14] W. J. Frith, P. D'Haene, R. Buscall, and J. Mewis, J. Rheol. **40**, 531 (1996).
[15] P. G. J. Van Dongen, Ph.D. thesis, Rijksuniversiteit Utrecht, 1983.
[16] M. von Smoluchowski, Z. Phys. Chem. **92**, 129 (1917).
[17] M. H. Ernst, *Fractals in Physics* (North-Holland, Amsterdam, 1986), p. 289.
[18] E. J. Hinch, *Perturbation Methods* (Cambridge University Press, Cambridge, England, 1991).